



Multi-generational carbonate assemblages in martian meteorite Allan Hills 84001: Implications for nucleation, growth, and alteration

Catherine M. CORRIGAN*[†] and Ralph P. HARVEY

Case Western Reserve University, Department of Geological Sciences, 112 A. W. Smith Building, 10900 Euclid Avenue, Cleveland, Ohio 44106–7126, USA

[†]Present address: Department of Mineral Sciences, National Museum of Natural History, Smithsonian Institution, Washington D.C. 20560–0119, USA

*Corresponding author. E-mail: corrigan.cari@nmnh.si.edu

(Received 04 February 2003; revision accepted 15 December 2003)

Abstract—The carbonate mineralogy of several complex carbonate-rich regions in Allan Hills (ALH) 84001 has been examined. These regions contain familiar forms of carbonate, as well as textural forms previously unreported including carbonate rosettes, planiform “slab” carbonates, distinct “post-slab” magnesites, and carbonates interstitial to feldspathic glass and orthopyroxene. Slab carbonates reveal portions of the carbonate growth sequence not seen in the rosettes and suggest that initial nucleating compositions were calcite-rich. The kinetically controlled growth of rosettes and slab carbonates was followed by an alteration event that formed the magnesite-siderite layers on the exterior surfaces of the carbonate. Post-slab magnesite, intimately associated with silica glass, is compositionally similar to the magnesite in these exterior layers but represents a later generation of carbonate growth. Feldspathic glasses had little or no thermal effect on carbonates, as indicated by the lack of thermal decomposition or any compositional changes associated with glass/carbonate contacts.

INTRODUCTION

Following its identification as a martian meteorite (Mittlefehldt 1994), Allan Hills (ALH) 84001 was rapidly recognized as being a very important sample of the martian crust. The most ancient of the martian meteorites (~4.5 Ga; Nyquist et al. 1995), ALH 84001's unique mineral assemblages record interactions with the environment of Mars in ways not provided by the younger martian meteorites (McSween and Treiman 1998). Petrologically, ALH 84001 is a cumulate orthopyroxenite (dominantly enstatite, $\text{Wo}_3\text{En}_{70}\text{Fs}_{27}$) with minor chromite, feldspathic glass, augite, apatite, and olivine (Mittlefehldt 1994; Harvey and McSween 1994). It is coarse-grained and has a cataclastic texture, indicating that it has been exposed to a series of impact shock events (Mittlefehldt 1994; Treiman 1995, 1998). This intense shock metamorphism has resulted in the presence of crushed zones, or granular bands, that contain crushed orthopyroxene, chromite, feldspathic glass, olivine, and other phases (Mittlefehldt 1994; Treiman 1995, 1998; Harvey and McSween 1996; McSween and Treiman 1998).

Many distinct histories have been suggested for ALH 84001 (e.g., Mittlefehldt 1994; Treiman 1995, 1998; Harvey and McSween 1996; Scott et al. 1997, 1998; Greenwood and

McSween 2001). Most agree on initial crystallization as part of a slow-cooling pluton and that the rock gained its current, highly fractured state during several post-crystallization impact events (e.g., Treiman 1998; Greenwood and McSween 2001). These impacts were separated temporally by some undetermined interval, as shown by the superposition of offset features in the secondary phases within fracture zones (Treiman 1995, 1998; McKay et al. 1997; Greenwood and McSween 2001). The resultant fractures provided conduits for the passage of fluids through the rock and allowed the development of secondary minerals within them.

The secondary minerals are of particular interest in ALH 84001 because they offer physical and chemical clues to past martian environments. Here, the phrase “secondary mineral” is used to describe any mineral that was not part of the original igneous assemblage. These include layered Mg, Fe, Ca-carbonates (calcite, dolomite-ankerite, magnesite-siderite), magnetite, sulfides (pyrite, pyrrhotite, and greigite), glass phases (including feldspathic and silica glasses), and rare phyllosilicates (Mittlefehldt 1994; Harvey and McSween 1996; McKay et al. 1996; Corrigan et al. 2000a; Brearley 2000; Greenwood and McSween 2001). Most of these secondary minerals are found within the crushed zones and associated fractures.

Carbonate minerals are the dominant secondary phase in ALH 84001, estimated to comprise between 0.46% and 1.0% of the rock (Romanek et al. 1994, 1995; Dreibus et al. 1994). They have been reported in a variety of settings and textures, from interstitial crack fillings to notably zoned clusters, semi-circular in cross-section, found in contact with orthopyroxene, feldspathic and silica glasses, and other minerals. Here, all circular or semi-circular carbonate assemblages will be referred to as rosettes.

ALH 84001 carbonate rosettes vary in composition concentrically, from Ca-rich near the center, through dolomite-ankerite (Mg-rich), to alternating magnesite-siderite layers at the outer edges (Mittlefehldt 1994; Harvey and McSween 1996; McKay and Lofgren 1997; Scott et al. 1997, 1998; Gleason et al. 1997). Siderite layers often contain fine, single-domain magnetite (Thomas et al. 1996; Bradley et al. 1996, 1998). These magnesite-siderite-magnesite layers will be referred to here as “MSM” layers.

Jull et al. (1995, 1997) analyzed isotopic compositions of carbonate minerals and concluded that they retain an extraterrestrial (martian) signature. A variety of ages for carbonate formation have been reported, from ~3.83 Ga to ~4.04 Ga (Turner et al. 1997; Borg et al. 1999). Most seem to accept these ages as coincident with the period of heavy bombardment in the inner solar system before ~3.8 Ga, though none of the carbonate ages are indisputable (Turner et al. 1997). In any case, carbonate formation clearly post-dates both initial igneous crystallization and an initial episode of fracturing by impact.

The exact processes responsible for carbonate formation are still in debate. Early attempts to understand these formation conditions arrived at widely varying conclusions, suggesting a complex history not fully explained by first-order solutions. Proposed formation scenarios include low temperature aqueous precipitation (Romanek et al. 1994; Treiman 1995; Hutchins and Jakosky 1997; Gleason et al. 1997; Valley et al. 1997; Leshin et al. 1998), evaporative processes (McSween and Harvey 1998; Warren 1998; Eiler et al. 2002a), high temperature reactions (Harvey and McSween 1996; Bradley et al. 1996, 1998; Leshin et al. 1998), and impact-induced melting (Scott et al. 1997, 1998). Recent experimental studies (Golden et al. 2000, 2001) confirm that low temperature precipitation (150 °C) from a saturated fluid followed by short-term heating can reproduce many of the carbonate features seen in ALH 84001.

Uncertainty also lies in whether there were single or multiple generations of carbonate formation (Mittlefehldt 1994; Treiman 1995; Harvey and McSween 1996; Greenwood and McSween 2001; Eiler et al. 2002b) and the role of post-precipitation alteration. Brearley (1998) suggested that some nm-scale mineralogy and textures in ALH 84001 result from thermal decomposition of pre-existing carbonate materials, particularly siderite decomposition to magnetite. Bradley et al. (1998) noted

similar textures. The experiments of Golden et al. (2000, 2001) showed that subsequent heating of carbonates formed in the laboratory (to 470 °C) was adequate to form magnetite crystals.

These previous studies suggest that the history of carbonate-bearing regions may have recorded a series of precipitation and alteration events, but the number and duration of events, and their nature, remain unclear. This paper reports the detailed textural and chemical relationships within several complex, carbonate-rich regions in ALH 84001, focusing primarily on carbonate minerals. Because these regions contain familiar forms of carbonate as well as more complete exposures of carbonate growth sequences, they can be placed into context with previous work, offering insight into the nucleation process for chemically zoned carbonates, and can lead to reassessment of proposed formation histories for carbonates in this rock.

METHODS

Two specially prepared thin sections of ALH 84001 were analyzed in detail. These sections, ALH 84001,302 (~2 mm × 4 mm) and ALH 84001,303 (~3 mm × 6 mm), were mounted in removable glue to ensure easy removal for TEM and destructive analyses. These sections were sliced from the same potted chip but differ in cross-sectional area and carbonate features. These 2 sections were selected from the 8 originally examined sections based on the presence of exceptionally large carbonate-bearing assemblages exhibiting a wide variety of textural relationships. The 2 studied regions share similar mineralogical and textural components, though relative abundances of key phases differ. These similarities suggest that the 2 regions have recorded similar (if not identical) processes that have been consistently observed throughout ALH 84001.

Preliminary electron microscopy was conducted at the University of Tennessee on the Cameca SX-50 microprobe and at NASA Johnson Space Center on the Cameca SX-100. Detailed spot analyses were conducted at the University of Chicago on the Cameca SX-50 microprobe. Carbonates were measured for Ca, Mg, Fe, and Mn using a 5 μm beam at 10 nA for 10 sec. An accelerating potential of 15 kV was used for all analyses.

TEXTURAL DESCRIPTION

The carbonate-bearing regions examined in this study exhibit a variety of textural relationships ranging from simple to complex, with carbonate and feldspathic and silica glasses being the most significant phases (Fig. 1). Carbonate occurs as the commonly described rosettes, as discrete, layered packages (here termed “slab” carbonates), as massive background fill (“post-slab magnesites”), and “interstitial” to feldspathic glasses and orthopyroxene. The latter 3 forms are

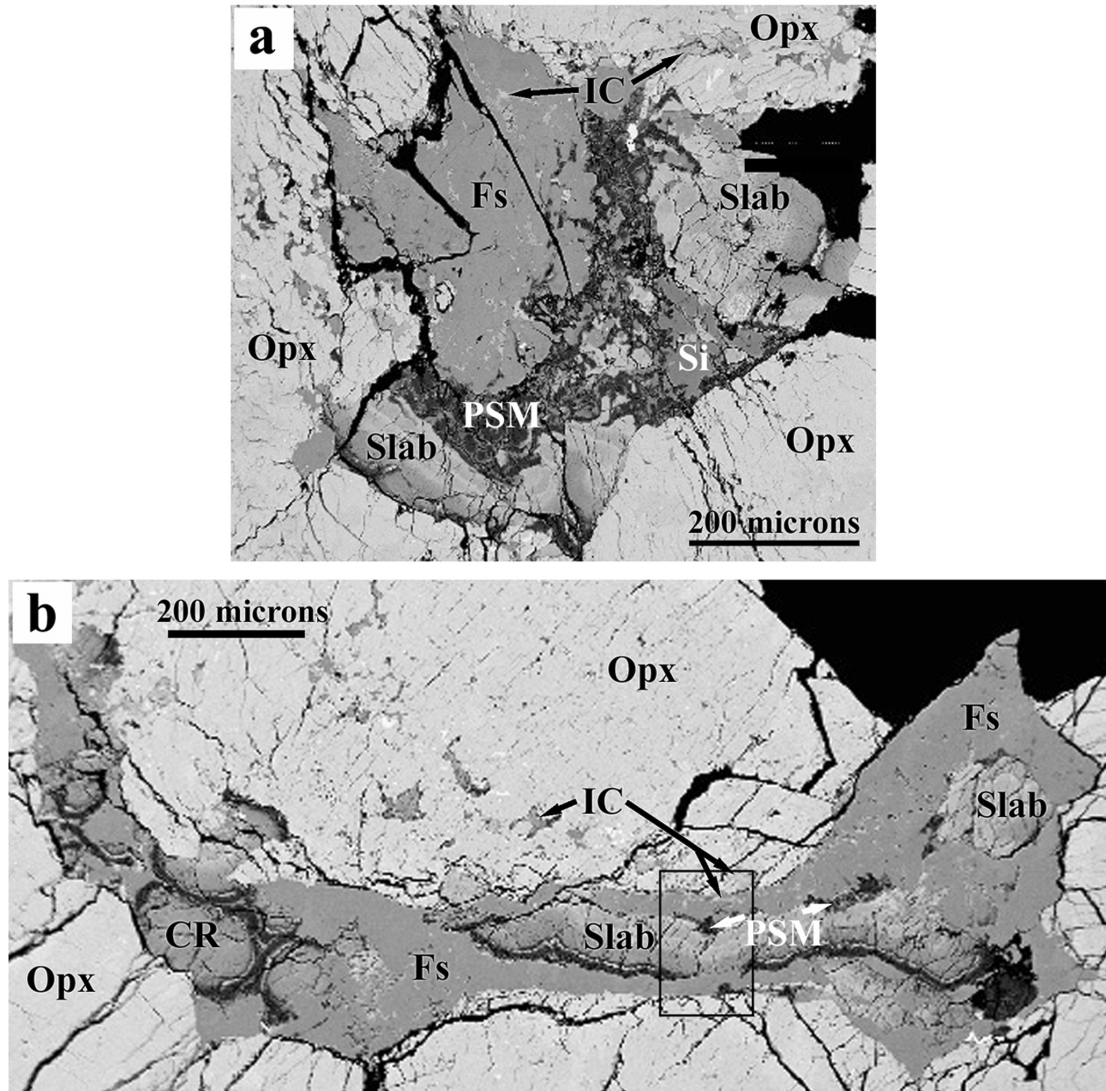


Fig. 1. a) BSE image of the region of secondary minerals in ALH 84001,302. Orthopyroxene (Opx) is the light gray phase surrounding the fracture. Slab carbonates (Slab) are found in the lower left and upper right corners of the region. The dark gray phase in the upper left is feldspathic glass (Fs). Carbonates found within orthopyroxene and feldspathic glass are collectively termed interstitial carbonate (IC). Dark, Mg-rich carbonates found between feldspathic glass and slabs are termed post-slab magnesite (PSM) and are often mixed with silica glass (Si) and other carbonate. The black regions on the right are the voids at the edges of sectioned rock material; b) BSE image of the region of secondary minerals in ALH 84001,303. In addition to the labeled phases described above, this region contains carbonate rosettes (CR) and extensive slab carbonate. The outlined region is enlarged and discussed in further detail in Fig. 5.

new classifications/terminology encompassing previously reported carbonate textures. For example, carbonates somewhat similar to slab carbonates are present in Greenwood and McSween (2001, their Fig. 9), Shearer and Adcock (1998, their Fig. 1), and Scott et al. (1998, their Fig. 1g) but are not studied in detail. Lacy carbonates from McKay et al. (1997), also seen in Greenwood and McSween (2001), would be categorized as interstitial here.

Rosettes

Rosettes were found only in ALH 84001,303 (Fig. 1).

These rosettes are identical to those described and analyzed in many previous studies of ALH 84001, with semi-circular cross-sections and distinct, consistent, and concentric chemical zoning. This zoning includes alternating magnesite-siderite-magnesite (MSM) layers on the outer portions of the carbonate sequence. The rosettes are in contact with both orthopyroxene and feldspathic glass. Feldspathic glass/carbonate contacts are sharp, and mineralogical associations existing at these contacts vary with location. In this section, rosettes vary in appearance from fractured and intact to broken up and dispersed (Fig. 1b). Fractures within the rosettes tend to crosscut the carbonate haphazardly (i.e., are

not dictated by chemical or textural variations) and do not extend into feldspathic glasses.

Slab Carbonates

A previously observed but undescribed form of carbonate, here termed “slab” carbonate, figures prominently in both study regions (Figs. 1 and 2). These slab carbonates are elongate packages that conform to fracture faces and exhibit chemical zoning distinctly visible in BSE images (Figs. 1 and 2), duplicating zoning commonly seen in rosettes. This zoning, however, is parallel to the faces of the slab (instead of concentric around a central point) and apparently exhibits a more complete chemical zoning record with sharper, more visible contacts between compositional zones (Figs. 2a and 2b). Slab carbonates include a thin, Ca-rich layer (bright in BSE) at one edge and the familiar MSM layers at the opposite edge, with 3 consistently distinct layers found between (Fig. 2a). The thickness of each layer appears relatively consistent, both along the extent of a single slab as

well as between slabs. Slab carbonates are typically highly fractured in a manner indistinguishable from that seen in rosettes, with fractures generally crossing all layers.

Like rosettes, slabs show no obvious preferential association with specific mineral species. They are found in contact with orthopyroxene, feldspathic glass, and other carbonate. In ALH 84001,302, slabs are in contact with both post-slab magnesite and orthopyroxene. In ALH 84001,303, slabs are in contact with both orthopyroxene and feldspathic glass, with a small amount of silica glass and post-slab magnesite along one edge of the large slab.

Post-Slab Magnesite

The regions studied here contain near Mg-end member carbonate that is texturally distinct from carbonate in rosettes or slabs. These appear black in BSE images (Figs. 1 and 2) and may be similar to those described by Romanek et al. (1995). We refer to these carbonates as “post-slab magnesites,” as we believe they formed as a distinct generation, post-dating zoned

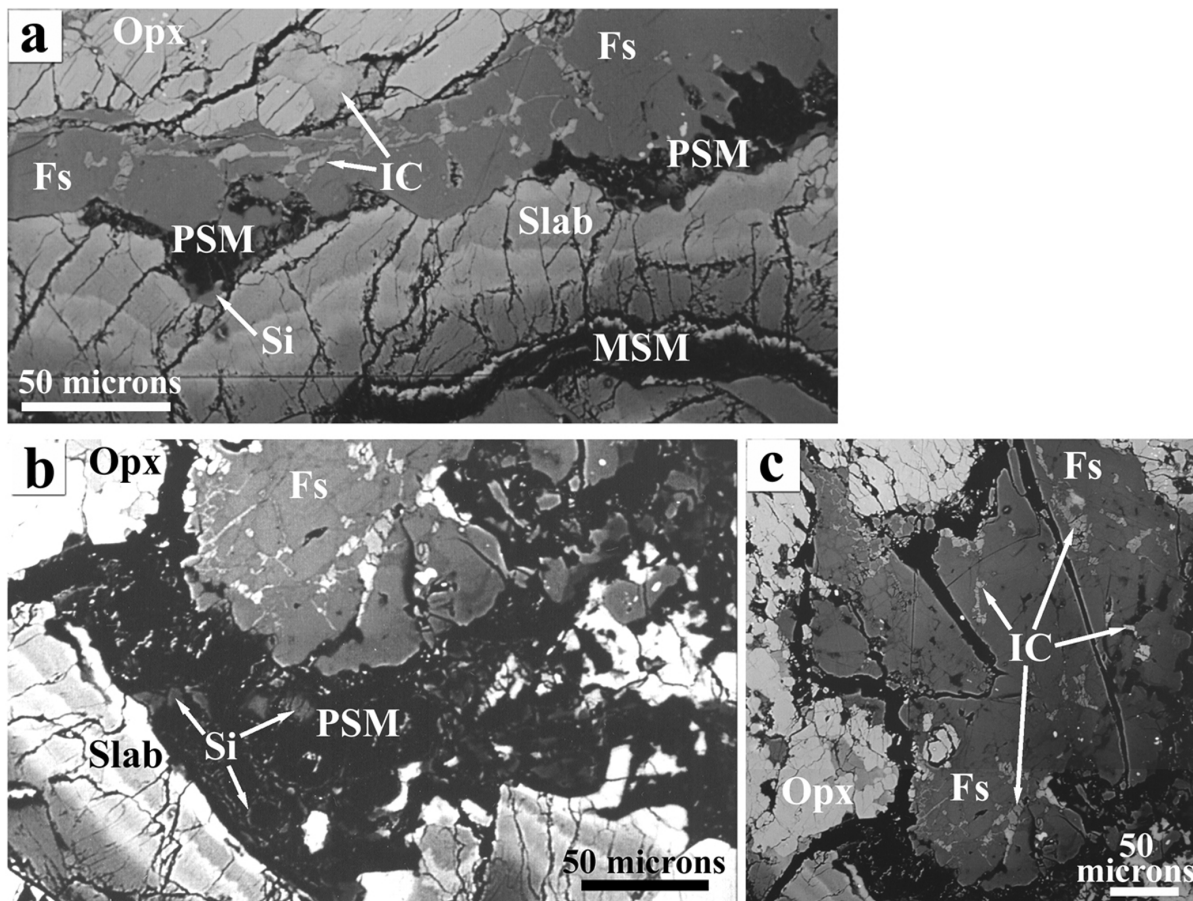


Fig. 2. BSE images of: a) ALH 84001,303 showing slab carbonate (Slab), post-slab magnesites (PSM), silica glass (Si), and magnesite-siderite-magnesite rims (MSM). Orthopyroxene (Opx) is present at the top of the image. Interstitial carbonates (IC) can be seen mixed with both orthopyroxene and feldspathic glass (Fs); b) post-slab magnesite in ALH 84001,302—close up showing blebbly texture of carbonate, silica glass rims around black carbonate blebs, and larger blebs of silica glass. This image was contrast enhanced to better show the mottled texture within the post-slab magnesite region; c) interstitial carbonate (IC) within feldspathic glass in ALH 84001,302.

slabs, rosettes, and MSM layers (see later discussion). Evidence that these carbonates are texturally distinct from rosettes or slabs is especially visible in ALH 84001,302 (Figs. 1a and 2b), where post-slab magnesite fills most of the space between slab carbonates and feldspathic glass. The post-slab magnesites occur as numerous blebs or grains. Individual blebs are semi-circular in cross section but show no evidence of being the outer edges of rosettes, as they are smaller (~50 μm ; rosettes range from ~100–250 μm ; Mittlefehldt 1994) and more uniform in size. These carbonates entrain small fragments of other minerals including other carbonates. Post-slab magnesites have a fracturing habit different from the zoned carbonates, with fractures formed around individual blebs and rarely crossing through them.

Post-slab magnesite also has an unusual relationship with silica glass. In ALH 84001,302 (Fig. 2b), silica glass is associated with fractures surrounding post-slab magnesite blebs, often forming rims around the blebs. Silica glass also occurs as larger irregular blebs (~100 μm diameter) surrounded by the magnesites (Fig. 2b). In ALH 84001,302 (Fig. 1a), post-slab magnesite lies between the thickly layered slab and feldspathic glass and is intermingled with elongated stringers of silica glass. Post-slab magnesite is found in ALH 84001,303, lying on the high-Ca edge of the slab carbonate (Figs. 1b and 2a), again in contact with silica glass and mixed with fragments of other phases. Post-slab magnesites are physically intermixed with the feldspathic glasses at the contacts between the two in both thin sections (Fig. 1).

Interstitial Carbonates

We have chosen to treat carbonate interstitial to larger domains of other minerals (particularly feldspathic glass and comminuted orthopyroxene) as a separate group. Feldspathic glasses, which account for a significant portion of the mineral inventory in these regions, are less fractured than is typically described for the bulk of ALH 84001 (McKay et al. 1998) and often exhibit a blebby texture, with convex, bulbous surfaces and lobate edges. While McKay et al. (1998a) reported silica rich veinlets in textures that appear similar to those seen here (Figs. 2a and 2c), these sections instead exhibit carbonate minerals between the glass blebs. These carbonates vary in form from stringers, to lithic fragments, to surface coatings similar to lacy carbonates seen by McKay et al. (1997) and Greenwood and McSween (2001, their Fig. 5). These peculiar textures are most evident in the feldspathic glass in ALH 84001,302 (Fig. 2c) and above/between the slabs in ALH 84001,303 (Figs. 1b and 2a). The simplest explanation for these interstitial textures is that they represent carbonate mechanically entrained by feldspathic glass.

Carbonates also appear in the interstices of the orthopyroxene surrounding the secondary mineral regions. These carbonates are similar in appearance to those found entrained within feldspathic glasses (though are generally

larger occurrences) and to those in orthopyroxene in numerous other studies (i.e., Schwandt et al. 1999; Eiler et al. 2002b).

COMPOSITION OF CARBONATES

Ternary Compositions (Mg, Ca, Fe)

Figure 3a shows ~800 carbonate analyses from these sections. The results of these new analyses overlap and extend compositional ranges previously reported for ALH 84001 carbonates (Mittlefehldt 1994; Harvey and McSween 1996; Scott et al. 1997, 1998; Leshin et al. 1998; and Eiler et al. 2002b). These new data show a much more continuous compositional trend filling gaps seen in previous work, including significant proportions of high-Ca carbonate seen only sporadically in previous studies.

As discussed in previous studies, the carbonate compositions found in ALH 84001 may actually be metastable. Note that the carbonates analyzed here are microcrystalline, and therefore, the size of the crystals may be smaller than the analyzed volume of the microprobe, possibly providing a somewhat inaccurate view of the compositions of individual grains.

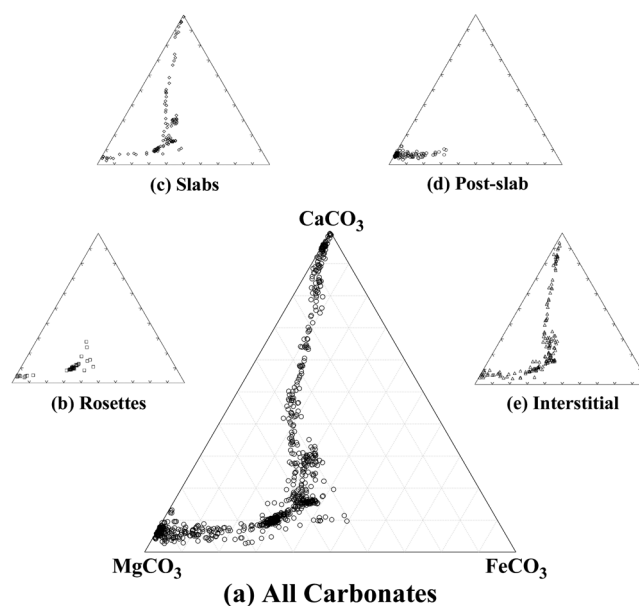


Fig. 3. Ternary diagrams of major element compositions of: a) all carbonates measured in ALH 84001,302 and ALH 84001,303; b) analyses of carbonate rosettes. Compositions from the interiors (more central to the ternary) are clearly distinguishable from those in the MSM rims (MgCO_3 apex); c) analyses of slab carbonate. These carbonates span the entire range seen in (a); d) analyses of interstitial carbonate. These also span the entire range of compositions; e) analyses of post-slab magnesites. As their name implies, these cluster in the Mg-carbonate apex of the diagram, though they do reach farther toward intermediate compositions than do the MSM rims seen in (b). All data are plotted as molar abundances of MgCO_3 , CaCO_3 , and FeCO_3 projected from MnCO_3 .

Manganese in Carbonates

Manganese is recognized as a minor constituent of ALH 84001 carbonates (Mittlefehldt 1994; McKay et al. 1996; Eiler et al. 2002b). Zoning of Mn/Fe has been reported across the rosettes, with cores enriched in Mn as well as Ca (Mittlefehldt 1994; Treiman 1995). In general, carbonates in this study show a positive correlation between MnCO_3 and CaCO_3 , though carbonates in the middle layers of the slabs exhibit elevated MnCO_3 (Fig. 4). Curiously, the high-Ca layers in ALH 84001,302 have lower MnCO_3 than those in ALH 84001,303, represented by the 2 clusters of high-Ca carbonate in Fig. 4. Magnesites from MSM rims and post-slab magnesites are Mn-poor (Fig. 4).

COMPOSITIONAL RELATIONSHIPS TO TEXTURES

Rosettes

The carbonate rosettes analyzed in this study are texturally and chemically indistinguishable from those examined in previous studies (Fig. 3b). Typical rosette compositions can be seen in Table 1. The most Ca-rich compositions of rosettes are consistently located near their centers, and MSM sequences are found around the rims, consistent with previous studies. MnCO_3 abundance in rosettes is low (<2 mol%; Fig. 4).

Slab Carbonates

Compositions of slab carbonates differ from rosettes only in that they exhibit a wider range of values, varying in a nearly continuous sequence across the ternary (Fig. 3c). The sharp boundaries between layers seen in BSE images (Figs. 1, 2a, and 2b) also correspond to visible compositional changes. Point analyses from 14 transects were constructed approximately perpendicular to zoning across slab carbonates in ALH 84001,303 (Fig. 5) and ALH 84001,302, revealing a consistent sequence of compositional variation (Table 2). This suggests that the compositional sequence seen in carbonate rosettes is a subset of that seen in slab carbonates.

Compositions (Table 2) across carbonate slabs (from Layer "A" to Layer "D"; Fig. 5) change from high-Ca carbonates (Layer "A"), through continually decreasing

CaCO_3 compositions (accompanied by increasing MgCO_3 and FeCO_3 abundance), to very low-Ca compositions (Layer "D"). The alternating high-Mg, high-Fe MSM layers are found at the end of this sequence (Fig. 5) and form clusters of points in the MgCO_3 apex (magnesite) of the ternary (Fig. 3c) and furthest toward the FeCO_3 apex (siderite).

Post-Slab Magnesite

These massive, space-filling carbonates exhibit predominantly Mg-rich compositions (Table 1; Fig. 3d). The post-slab magnesite spans a wider compositional range than magnesites in the MSM layers, from nearly pure MgCO_3 to intermediate compositions. MnCO_3 contents of post-slab magnesites are low, consistently <~1% (Fig. 4).

Post-slab magnesites show no recognizable zoning or other chemical trends. Compositions do not vary with respect to distance from any particular center point nor do they vary dependent on proximity to other mineral phases. High-Ca phases appear to have been mechanically entrained within the post-slab magnesite (Figs. 2a and 2b).

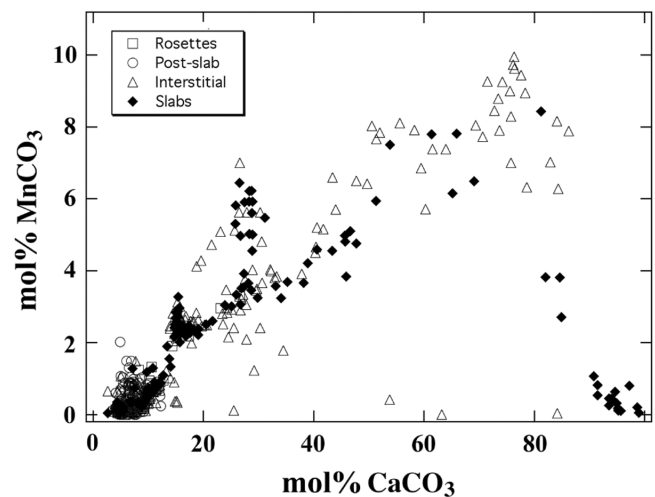


Fig. 4. MnCO_3 versus CaCO_3 within ALH 84001 carbonates of different textural types. Interstitial carbonates (Δ) and slab carbonates (\blacklozenge) span the entire compositional range, though hi-Ca slab carbonates show variations with MnCO_3 . Post-slab magnesite (\circ) and rosette (\square) compositions are restricted to the low- CaCO_3 / MnCO_3 corner of the diagram. Compositions are presented in mol% carbonate.

Table 1. Representative compositions of ALH 84001 carbonates from this study.^a

	Rosettes				Post-slab magnesite				Interstitial carbonates			
	1	2	3	4	5	6	7	8	9	10	11	12
Analysis	303-048	303-071	303-079	303-088	302-424	302-441	303-157	303-265	302-004	302-325	303-102	303-245
CaCO_3	14.978	11.862	9.909	9.595	5.788	5.424	6.607	5.145	84.349	29.533	10.390	73.488
MgCO_3	45.876	55.973	59.882	59.460	93.735	94.038	92.456	93.356	6.886	42.898	59.268	12.431
FeCO_3	36.594	31.372	29.591	30.498	0.435	0.518	0.801	1.408	2.491	24.115	29.639	5.301
MnCO_3	2.552	0.794	0.618	0.447	0.042	0.020	0.136	0.091	6.274	3.454	0.704	8.780

^aCompositions are presented in mol% carbonate.

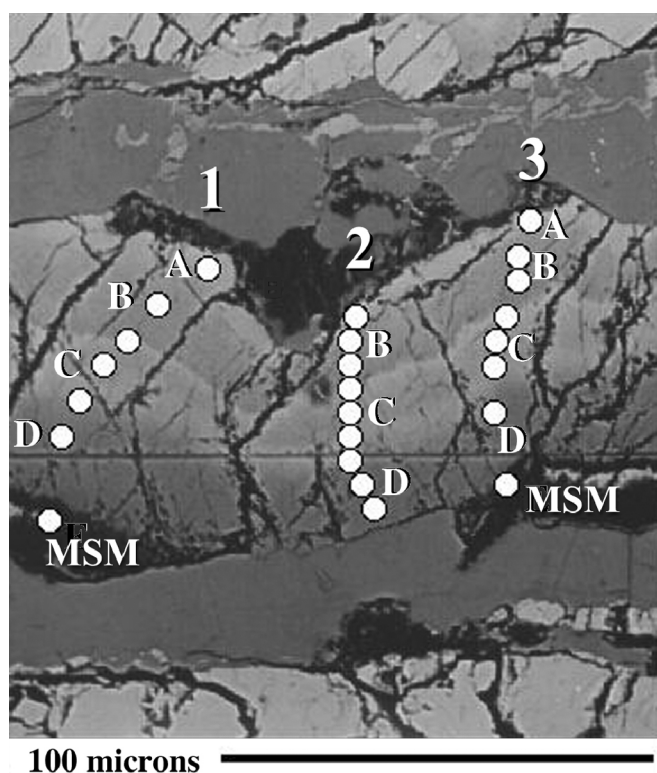


Fig. 5. Enlarged region of ALH 84001,303 showing locations of profiles across slab carbonates. Each point represents an individual analysis. Layers (A–D) are designated for ease of discussion in the text and to demonstrate the compositional variation across a slab. Compositions from each profile (labeled as 1–3) beginning at the “top” of the slab relative to this image are displayed in Table 2. Profiles across slab carbonates were also analyzed in ALH 84001,302 with consistent results.

Interstitial Carbonates

Interstitial carbonates are not chemically distinct from slabs, rosettes, or post-slab magnesites. Their compositions span nearly the entire range seen in Fig. 3a, though most are intermediate (Fig. 3e). Interstitial carbonates exhibit only small variations in composition within individual occurrences; most are too limited in size for significant variation to be apparent. Manganese content of interstitial carbonates spans the entire range seen in the above textural occurrences (Fig. 4).

Interstitial carbonates found in feldspathic glasses vary in chemistry with location. For example, within feldspathic glass in ALH 84001,302, carbonates near the contact with post-slab magnesites (Figs. 1a and 2b) contain higher calcium compositions than those found closer to orthopyroxene (Figs. 1a and 2c). In ALH 84001,303, carbonates interstitial to feldspathic glass (Figs. 1b and 2a) vary between being relatively Ca-rich and intermediate in composition. Post-slab magnesite material occurs in the interstices of feldspathic glass but only at the contacts between the two. Variations in the chemistry of interstitial carbonates suggest that the enclosed

Table 2. Representative compositions of ALH 84001,303 slab carbonate traverses.^a

Analysis	CaCO ₃	MgCO ₃	FeCO ₃	MnCO ₃
Traverse 1				
303-147	69.076	16.958	7.476	6.490
303-148	38.181	38.578	19.573	3.667
303-149	28.753	36.548	28.476	6.223
303-150	17.387	47.278	32.859	2.476
303-151	14.967	47.325	34.868	2.840
303-152	11.125	58.678	29.286	0.912
303-268	3.320	92.444	4.133	0.103
Traverse 2				
303-288	65.165	19.500	9.180	6.154
303-287	43.359	35.535	16.548	4.558
303-286	26.723	45.147	25.062	3.067
303-285	28.843	39.293	27.308	4.556
303-284	25.096	42.794	29.095	3.015
303-283	14.989	47.296	35.026	2.689
303-282	10.507	60.184	28.634	0.675
303-156	10.279	60.288	28.742	0.691
303-281	9.302	61.855	28.504	0.338
Traverse 3				
303-292	65.945	17.443	8.801	7.810
303-293	40.593	37.381	17.439	4.587
303-294	15.724	52.655	29.606	2.015
303-295	28.252	37.438	28.387	5.923
303-296	16.784	49.642	31.396	2.179
303-297	14.729	49.319	33.537	2.415
303-298	9.923	61.437	27.962	0.677
303-269	4.359	94.908	0.569	0.165

^aCompositions expressed in mol% carbonate. Compositions correspond to traverse points seen in Fig. 5 starting at the top of the slab in each traverse relative to the image and moving toward MSM rims at the bottom.

carbonates are a combination of all observed carbonate sources and do not represent unique mineral phases.

Chemical compositions of carbonates filling voids in the orthopyroxene do not vary greatly within individual occurrences, though they do vary between occurrences. The interstitial carbonates within orthopyroxene likely formed during the same event as the slabs and rosettes.

DISCUSSION

Nucleation

Mineral growth in most natural precipitation systems is kinetically controlled (Tromp and Hannon 2002). Under such conditions, precipitation of carbonate minerals is dependent on fluid composition, time, temperature, and available space. Very minor changes in super-saturated fluid compositions produce much larger changes in precipitate chemistry (Woods and Garrels 1992). Where nucleation is limited, these chemical changes are typically manifested as

ring-like patterns of microcrystalline growth in the resulting precipitates, often containing wide compositional variation concentric around a small number of nucleation points (McKay and Lofgren 1997). The smoothly varying carbonate compositions that indicate the presence of microcrystalline, metastable phases, and limited numbers of nucleation sites (i.e., carbonate rosettes) are clear signatures of kinetically controlled carbonate growth in ALH 84001. The concentric zoning is probably due to sequential chemical changes during growth from a super-saturated fluid, as suggested by many of the proposed precipitation scenarios for ALH 84001 carbonate (e.g., Golden et al. 2000, 2001). The tendency of rosettes to fill all available space and the absence of a favored substrate material also suggest that they grew outward from single nucleation points under kinetic control and are not replacements of pre-existing phases (Harvey and McSween 1996; McKay and Lofgren 1997; Golden et al. 2000, 2001).

The textures of microcrystalline slab carbonates, which exhibit the same zoning sequence as rosettes, are also consistent with formation under kinetically controlled conditions. Slab carbonates show visible zoning parallel to fracture surfaces, suggesting nucleation from numerous, closely spaced points on a surface instead of from widely spaced individual points. The identical zoning in rosettes and slabs suggests that they formed during the same growth event; the distinction between the 2 forms must, therefore, be related to limits of nucleation.

One factor that can potentially explain the coexistence of the 2 forms of carbonate is fracture volume. Nucleation is a difficult process to initiate, generally requiring a high concentration of available nucleation sites (mineral surface defects, pre-existing crystallites, and/or regions of dense cation concentration serve as nucleation points). The number of these sites is dependent on spatial volume; a larger volume can contain more fluid and more “seeds” of crystallization to facilitate nucleation. In a larger fracture, a larger volume of fluid would, upon evaporation, translate to a larger population of nucleation sites when these “seeds” (which may have initiated growth while suspended within the fluid) are reduced to fracture walls as fluid disappears. This would produce a higher density of nucleation sites that, in turn, would result in crystals growing in closer proximity, eventually coalescing and forming larger, extended carbonates. Therefore, when there is sufficient fluid volume, slabs will form, while rosettes will form when the volume is limited.

These differences in nucleation suggest that slab carbonates are of particular value in understanding the sequence of carbonate crystallization. The semi-planar geometry of slab carbonates offers a geometric advantage in that a random slice through a slab is more likely to intersect the full range of compositions present in 3 dimensions than is a slice through a semi-spherical or pancake-shaped

rosette. Slab carbonates should, thus, provide a more complete history of carbonate formation, exposing compositions representative of early stages of formation rarely seen in rosettes. Assuming that MSM layers are the exterior (altered) layers of rosettes (Brearley 1998), the high-Ca carbonates on the opposite face of the slabs should represent the earliest compositions (possibly even original nucleating compositions). This is only the case, however, if subsequent movement of slabs away from nucleation surfaces has kept the faces very nearly parallel (i.e., the slabs are not rotated out of the view of the thin section) and if subsequent events have not altered or destroyed these earliest carbonates.

PROPOSED SEQUENCE OF EVENTS

We propose the following history of carbonate formation in ALH 84001. Initial formation of the rock as a cumulate orthopyroxenite was followed by impact events resulting in an initial set of fractures within the rock (Mittlefehldt 1994; Treiman 1998). A carbonate growth stage later occurred during which rosettes and slab carbonates were precipitated into the fractures from fluids that were super-saturated in carbonate components. Rosettes arose from isolated nucleation sites in relatively small fractures, forming pancakes where perpendicular growth was limited and more spheroidal shapes where space allowed. Slabs nucleated in rare, larger fractures. The earliest formed carbonates were Ca-rich, but crystallization progressed toward more Mg- and Fe-rich compositions. Occasional recharge of fluids during carbonate growth altered the cation concentrations resulting in the variable compositions visible as zones in BSE (Figs. 1 and 2). This is likely similar to the “occasional oscillations back to more calcic compositions” inferred by McKay and Lofgren (1997).

Magnesite-Siderite-Magnesite Rims

In this proposed history, the formation of MSM layers is the first significant event to have affected pre-existing carbonate minerals. Observations from this study are consistent with the suggestion by Brearley (1998) and others that MSM layers were formed by thermal decomposition during a high-temperature, impact-induced event. This hypothesis is also supported by the porous texture of carbonate seen on the nanometer scale, where voids are often found associated with magnetite and other Mg and Fe phases (Corrigan et al. 2000b; Barber and Scott 2001; Scott and Barber 2002). Magnetite is thought to have formed from thermal decomposition of siderite at high temperatures, since siderite is typically stable only below 550 °C (Essene 1983) and has been seen to decompose at temperatures as low as 385 °C (Gallagher et al. 1981). Experiments conducted by Golden et al. (2001) showed magnetite formation from

synthetic siderites heated briefly to 470 °C. Koziol and Brearley (2002) conducted similar experiments, heating various compositions of Mg-Fe carbonates to 470 °C for short periods in both ambient and reduced fO_2 environments. Decarbonation and magnetite formation occurred in all samples. Shock experiments by Bell et al. (2002) show that at least 49 GPa of pressure was reached in ALH 84001, since siderite shocked to these pressures showed evidence of devolatilization and transformation of parent carbonate to oxides seen in ALH 84001 carbonates. Langenhorst (2000) suggested that shock pressures as high as 60 GPa were reached in the rock, and Stöffler (2000) reported that pressures this high should produce temperatures exceeding 600 °C. It seems, then, that temperatures and pressures may have been sufficiently elevated during this event to decompose carbonate minerals.

The chemistry, mineralogy, and textures of carbonate in this study lead us to favor a thermal event as the formation mechanism for MSM layers rather than singular, dramatic changes in fluid chemistry. Formation of the MSM layers may have involved replacement or dissolution and redeposition of carbonate materials. We suggest that this event caused the conversion of an exterior, Mg- and Fe-rich carbonate

composition (Fig. 6) into the residual MSM layers. The original trend toward lower Ca compositions with relatively constant proportions of Fe and Mg (slabs) was replaced with carbonates of relatively constant Ca and widely varying proportions of Fe and Mg (MSM). This event would have occurred with the earliest slab carbonates still attached to nucleation surfaces, as these innermost compositions appear to be unaffected by alteration. In addition, MSM layers are found concentric only around the exteriors of zoned carbonates, which would have required free space between these surfaces and the fracture walls, present either because carbonate growth did not completely fill the fracture or because the fracture was later widened, possibly during an impact event. This widening need not have been significant—just enough to let fluids move through to the carbonates. Interior carbonates may have had a more cohesive bond with the orthopyroxene walls, as they were not peeled away, exposed, or altered during such an event.

Thermal decomposition has numerous implications for carbonates that have not yet been fully explored. Complete decomposition of slab carbonates should result in the presence of Fe, Mg, Ca, and Mn-oxides and the absence of recognizable carbonate minerals. Though recent works by Barber and Scott (2001) and Scott and Barber (2002) report the presence of MgO (periclase) associated with magnetite in the MSM rims, carbonates are also still present in the rims, indicating that thermal decomposition was incomplete, likely part of a short-lived, impact-induced event. After removal of Fe from the carbonates, expected compositions would lie along the Ca-Mg boundary of the ternary (Fig. 6, “4a”). Ca-oxides are not present, however, and we see the horizontal trend (Fig. 6, “4b”), which is less linear and depleted in Ca. Therefore, Ca and Mn may have been lost during the thermal decomposition process. Alternatively, the exterior composition being altered in this event originally contained less Ca than previously thought (Harvey and McSween 1996; Corrigan and Harvey 2002), and exterior carbonate compositions have evolved “backward” toward the higher Ca abundances seen just inside the MSM layers.

While invocation of a high temperature thermal decomposition event has significant implications for the mineralogical and chemical composition of the carbonates, it must also fit constraints provided by the isotopic data for ALH 84001 carbonates. Current oxygen isotope analyses of carbonate rosettes and interstitial carbonates show that the interior carbonates have the lowest $\delta^{18}O$ values, while exterior carbonates have the highest (Valley et al. 1997; Leshin et al. 1998; Saxton et al. 1998; Eiler et al. 2002b), implying decreasing temperature during carbonate formation. If correct, this is inconsistent with our model. We caution, however, that existing isotopic data is largely restricted to the well-documented rosettes and interstitial carbonates, while few, if any, measurements exist from these newly-defined carbonate occurrences.

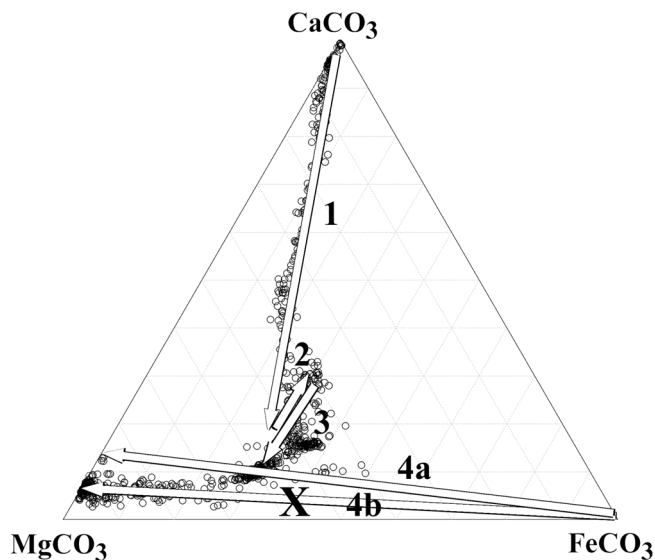


Fig. 6. Carbonate growth trends and possible alteration in ALH 84001. Arrow 1 shows the initial growth trend starting at the $CaCO_3$ apex and continuing with decreasing calcium. An influx of fluid enriched in Ca, Fe, and Mn disrupted the smooth transition from Ca-rich to Ca-poor carbonate (arrow 2). The pattern of decreasing Ca and increasing Mg content in carbonate growth resumed after this influx (arrow 3). The carbonates in group D (Fig. 5) were either the final composition of carbonate growth or a composition remaining after decomposition of a more Ca-poor carbonate (possibly of composition X), forming MSM layers (4a, 4b). 4a represents an alteration that removed Fe components from a carbonate of current exterior (inside-MSM) composition. 4b represents an alteration that removed Fe components from a pre-existing (now removed) carbonate composition containing less calcium than current exterior compositions.

Post-Slab Magnesites

Post-slab magnesites comprise a significant volume of material in these thin sections, particularly in ALH 84001,302, suggesting that their formation event may have been significant. Textures suggest that post-slab magnesites represent a distinct precipitation event that took place after the MSM sequences formed and before feldspathic glass intruded. Most fractures crossing slab carbonates and MSM layers do not cross into post-slab magnesites. Entrainment of slab carbonate material into post-slab magnesites in ALH 84001,302 (Fig. 1a) also suggests that these magnesites formed after rosettes and slabs.

Unlike MSM bands, post-slab magnesites are found in contact with the oldest (earliest formed) slab surfaces. The Ca-rich edges of the slab must have been detached from their original nucleation surfaces, allowing space for post-slab magnesite to precipitate. The occurrence of post-slab magnesite on the same high-Ca face of slab carbonates in ALH 84001,303 (Fig. 2b) indicates that post-slab magnesite was precipitated before the 2 pieces of slab were separated from one another.

Post-slab magnesites are also physically mixed with silica glasses, suggesting that either the 2 phases were emplaced during the same event or silica glass precipitated after post-slab magnesite. Silica glass both surrounds blebs of post-slab magnesite and forms individual occurrences within it in both studied regions (Figs. 2a and 2b). Fracture analysis is difficult, as fractures do not cross-cut both phases but tend to form around magnesite blebs, generally through silica occurrences. Though observed in other studies of ALH 84001 carbonates (Valley et al. 1997), neither of these phases intrudes into slab carbonates or rosettes in these thin sections, though they are both found in contact with these phases. Recent oxygen isotope analyses from Greenwood and McKeegan (2002) suggest that carbonate and silica glasses did not form in equilibrium, but whether the carbonate they are discussing is the same as our post-slab magnesites is not clear.

Chemically, MSM magnesites and the post-slab magnesite are similar (Figs. 3c and 3d), suggesting that they formed either by similar processes or that they represent 2 stages of a single event. The first of these events decomposed existing carbonates and deposited the MSM rims, while the second precipitated the chemically similar post-slab magnesites and silica glass, filling in the trend with compositions lost during the first event. An influx of silica to the fluid (possibly leached from the feldspathic glass) during either the second or a later impact event may have allowed the formation of amorphous silica as the latest phase in this stage, precipitating between rosettes and around blebs of post-slab magnesite (Figs. 2a and 2b). Isotopic analysis of MSM rims, post-slab magnesite and silica glasses should shed light on the relationship of these phases, as the number of events that transpired to form them is currently unclear based on textural evidence alone.

In summary, the trend seen in Fig. 3a can be described as a depositional event (vertical portion of the trend) followed by 2 alteration events (MSM and post-slab magnesites). The latter may actually be a single, multi-staged event.

Feldspathic Glass

In both thin sections, there are numerous occurrences of zoned carbonates and post-slab magnesite entrained by feldspathic glass. In addition, locations exist where fractures transcend the boundaries between both types of carbonate but do not cross into feldspathic glasses. Based on these arguments, feldspathic glass was the last phase to enter these fractures, its intrusion implying yet another possible impact event. The bulbous texture and lobate contacts with post-slab magnesite (Figs. 1 and 2b) suggest that feldspathic glasses were mobile and flowed into these fractures. Feldspathic glass intrusion produced physical effects but did not seem to cause significant chemical changes. Glass intrusion further widened the fractures, entraining phases already present in fractures and further peeling some carbonates from their nucleation sites. The intrusion of feldspathic glass separated the slabs in ALH 84001,303, and the attached post-slab magnesites. These examples of carbonate minerals being sheared from their substrates by glasses echo those shown by Shearer and Adcock (1998). Interstitial carbonates, particularly those between the top of the slab and the orthopyroxene wall in ALH 84001,303, appear to have been entrained within the feldspathic glass during this event. These interstitial carbonates (Figs. 1b and 2a) correspond well to compositions on either side of the feldspathic glass. Greenwood and McSween (2001) suggest that carbonates similar to these grew around the feldspathic glass blebs and were decarbonated by a later heating event. This has not been ruled out as a way to explain the carbonates seen here, but the interstitial carbonates examined in this study show no systematic evidence of decarbonation at this scale. McKay et al. (1998b) report fractures within feldspathic glass filled with silica glass similar to those seen in post-slab magnesites in these regions. Silica-filled fractures in feldspathic glasses are not seen in these thin sections, though searching for such veins could provide a test as to whether or not feldspathic glass intruded at high-temperatures or was later infiltrated with silica-bearing fluids. From these sections alone, it would appear that silica-rich fluids infiltrated before feldspathic glass intrusion.

That the introduction of feldspathic glass into carbonate-bearing fractures was an agent of carbonate alteration has been suggested (Schwandt et al. 1999; Greenwood and McSween 2001). Evidence found in this study suggests that feldspathic glass is not responsible for decarbonation of pre-existing carbonate. The stratigraphy is incorrect for feldspathic glass formation simultaneously with or preceding MSM formation. MSM sequences are present around the

exterior of zoned carbonates, but neither slabs nor rosettes are consistently altered everywhere they are in contact with feldspathic glass, contrary to what would be expected if feldspathic glass was responsible for MSM formation. Numerous examples of unaltered slab carbonates are seen in contact with feldspathic glass in ALH 84001,303 (Figs. 1b and 2a). The variation in composition of carbonates interstitial to feldspathic glass is strong evidence that they are unaltered, mechanically entrained materials as opposed to post-intrusion precipitates. In addition, slab carbonates in ALH 84001,302 are not visibly in contact with feldspathic glass yet still exhibit MSM sequences.

Studies of glass rheology may provide a solution to this paradox. Although most researchers studying ALH 84001 assume that mobilization of feldspathic glass requires high

temperatures, experiments have shown that when silica glasses are exposed to high static pressures (MPa range), their viscosity can drop many orders of magnitude without significant temperature elevation (Rekhson et al. 1980; Mazurin et al. 1982). Subsequent shear then easily deforms the glass with little thermal consequence (Rekhson et al. 1980; Mazurin et al. 1982). Impact events generating 45–60 GPa of pressure (Bell et al. 2002; Langenhorst 2000) provide more than enough stress needed to reach this transition. As a result, feldspathic glass can flow on the mm scale (as suggested by textures seen in ALH 84001) in the absence of a thermal pulse. The impact event(s) that mobilized the feldspathic glasses seen in the regions studied here likely provided enough shear strength to allow the glass to flow into the fractures at low temperatures.

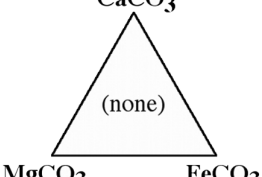
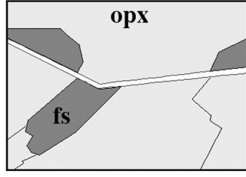
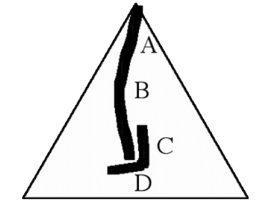
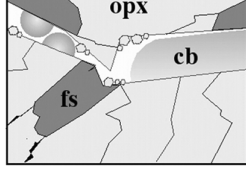
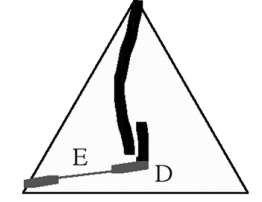
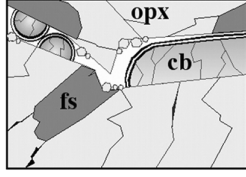
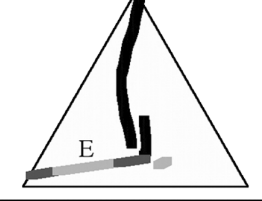
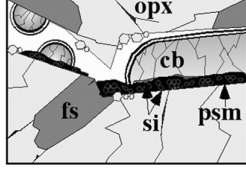
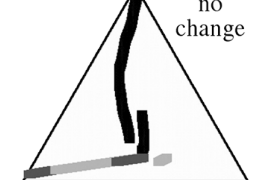
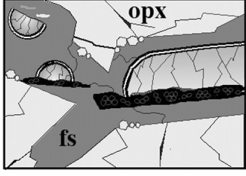
Event	Carbonate Chemistry	Textures
<p>~ Fracturing of original rock - feldspar focus of fracturing - feldspar to glass</p>	<p>CaCO₃</p>  <p>MgCO₃ FeCO₃</p>	
<p>~ Initial carbonate deposition - rosettes and slabs - groups A-C, D?</p>		
<p>~ MSM deposition - around rosettes and slabs - group E ~ Further fracturing and offset</p>		
<p>~ Opening of fracture ~ Post-slab magnesite & Si glass deposition - group E ~ Further fracturing</p>		
<p>~ Intrusion of feldspathic glass - shearing of cb from opx walls</p>	<p>no change</p> 	

Fig. 7. Proposed sequence of events relating to carbonate development in ALH 84001 in terms of chemistry and texture.

CONCLUSIONS

The carbonate-bearing regions examined here are unique in that they include observations of commonly studied rosettes and 3 newly described, petrologically distinct types (planiform “slabs,” secondary “post-slab magnesites,” and “interstitial” carbonates). Studying these carbonates in their surroundings offers valuable petrologic and chronologic context and provides a new baseline for many previously disparate observations.

Analyses of slab carbonates reveal a formation history (Fig. 7) that is clearly shared with that of the rosettes but includes well-exposed sections of earlier formed compositions rarely seen in spheriform carbonates. The chemical stratigraphy revealed by the slabs suggests that first generation carbonates were essentially calcite-rich, with Ca diminishing as crystallization proceeded toward intermediate compositions. This growth sequence was followed by an alteration event, presumably with a major thermal effect that decarbonated the FeCO₃ component of an exterior carbonate to produce the MSM sequence on the exposed surfaces of the pre-existing carbonates. While the complete nature of the MSM forming event is unclear, textures and chemistry suggest that it involved high-temperature decomposition of the exterior surface of pre-existing carbonates, producing oxides and charging the fluid with ionic Ca, Fe, Mg, and CO₂. This event was followed by redeposition of carbonates with varying Mg/Fe content (MSM sequences) and trapped Fe oxides as that liquid cooled and/or evaporated. After an undetermined interval, a reactivation of fractures detached slabs from surrounding walls, creating space for a new generation of carbonate precipitation (post-slab magnesite). The chemistry of these carbonates was essentially identical to the magnesitic portions of the MSM sequences (possibly precipitating from the same medium) and they show an intimate relationship with silica glass. After another undetermined interval, pre-existing feldspathic glasses were mechanically emplaced with little or no thermal effect on the carbonates, as suggested by the lack of thermal decomposition or any compositional changes associated with contact with the glass.

The presence of numerous, distinct generations of carbonate formation and relatively clear fracture chronology within carbonate further suggest that interactions between ALH 84001 and the crustal fluids of Mars were discontinuous and occurred only a few times over its 4.5 Ga history. The reactivation and remobilization of fluids (causing events such as MSM formation and precipitation of post-slab magnesite) and the fracturing within the rock were almost certainly impact driven. The evidence for punctuated, impact-driven interaction between rocks and fluids supports scenarios such as those of Segura et al. (2002), where large impacts created temporary hydrous environments, as opposed to those including large-scale, long-term hydrologic systems including oceans (Baker

et al. 1991; Clifford and Parker 2001). Therefore, unless ALH 84001 is a particularly rare, particularly pristine sample, the hydrosphere of Mars may not have interacted with the rocks as thoroughly as is sometimes assumed.

Acknowledgments—We would like to thank Craig Schwandt, Ian Steele, and Mini Wadhwa for their time and assistance with electron microprobe analyses. We would also like to thank Dr. Simon Rekhson of the Advanced Manufacturing Center at Cleveland State University for discussions on the properties and behaviors of silicate glasses. Many thanks to D. Mittlefehldt, T. Mikouchi, and an anonymous reviewer for insightful reviews that significantly improved this manuscript. This research was funded by the Ohio Space Grant Consortium, the Zonta International Foundation’s Amelia Earhart Fellowship, and NASA grant NAGS-11122.

Editorial Handling—Dr. David Mittlefehldt

REFERENCES

- Baker V. R., Strom R. G., Gulick V. C., Kargel J. S., Komatsu G., and Kale V. S. 1991. Ancient oceans, ice sheets, and the hydrological cycle on Mars. *Nature* 352:589–594.
- Barber D. J. and Scott E. R. D. 2001. Transmission electron microscopy of carbonates and associated minerals in ALH 84001: Impact-induced deformation and carbonate decomposition (abstract). *Meteoritics & Planetary Science* 36: A13–A14.
- Bell M. S., Schwandt C., Zolensky M. E., and Horz F. 2002. Experimental shock decomposition of siderite (abstract). *Meteoritics & Planetary Science* 37:A14.
- Borg L. E., Connelly J. N., Nyquist L. E., Shih C. Y., Wiesmann H., and Reese Y. 1999. The age of the carbonates in martian meteorite ALH 84001. *Science* 286:90–94.
- Bradley J. P., Harvey R. P., and McSween H. Y., Jr. 1996. Magnetite whiskers and platelets in the ALH 84001 martian meteorite: Evidence of vapor phase growth. *Geochimica et Cosmochimica Acta* 60:5149–5155.
- Bradley J. P., McSween H. Y., Jr., and Harvey R. P. 1998. Epitaxial growth of nanophase magnetite in martian meteorite Allan Hills 84001: Implications for biogenic mineralization. *Meteoritics & Planetary Science* 33:765–773.
- Brearley A. J. 1998. Magnetite in ALH 84001: Product of the decomposition of ferroan carbonate (abstract #1451). 29th Lunar and Planetary Science Conference. CD-ROM.
- Brearley A. J. 2000. Hydrous phases in ALH 84001: Further evidence for preterrestrial alteration and a shock-induced thermal overprint (abstract #1203). 31st Lunar and Planetary Science Conference. CD-ROM.
- Clifford S. M. and Parker T. J. 2001. The evolution of the martian hydrosphere: Implications for the fate of a primordial ocean and the current state of the northern plains. *Icarus* 154:40–79.
- Corrigan C. M., Harvey R. P., and Bradley J. P. 2000a. Phyllosilicate minerals in martian meteorite ALH 84001 (abstract). *Clay Mineral Society* 37:38.
- Corrigan C. M., Harvey R. P., and Bradley J. P. 2000b. Sodium-bearing pyroxene in ALH 84001 (abstract #1762). 31st Lunar and Planetary Science Conference. CD-ROM.
- Corrigan C. M. and Harvey R. P. 2002. Unique carbonates in martian

- meteorite Allan Hills 84001 (abstract #1051). 33rd Lunar and Planetary Science Conference. CD-ROM.
- Dreibus G., Burgele A., Jochum K. P., Spettel B., Wlotzka F., and Wanke H. 1994. Chemical and mineral composition of ALH 84001: A martian orthopyroxenite (abstract). *Meteoritics* 29:461.
- Eiler J. M., Kitchen N., Leshin L., and Strausberg M. 2002a. Hosts of hydrogen in Allan Hills 84001: Evidence for hydrous martian salts in the oldest martian meteorite? *Meteoritics & Planetary Science* 37:395–405.
- Eiler J. M., Valley J. W., Graham C. M., and Fournelle J. 2002b. Two populations of carbonate in ALH 84001: Geochemical evidence for discrimination and genesis. *Geochimica et Cosmochimica Acta* 66:1285–1303.
- Essene E. J. 1983. Solid solutions and solvi among metamorphic carbonates with applications to geologic thermobarometry. In *Carbonates: Mineralogy and chemistry*, edited by Reeder R. J. Washington D.C.: Mineralogical Society of America.
- Gallagher P. K., Warne S. St. J., and West K. W. 1981. Use of Mossbauer effect to study the thermal decomposition of siderite. *Thermochimica Acta* 50:41–47.
- Gleason J. D., Kring D. A., Hill D. H., and Boynton W. V. 1997. Petrography and bulk chemistry of martian orthopyroxenite ALH 84001: Implications for the origin of secondary carbonates. *Geochimica et Cosmochimica Acta* 61:3503–3512.
- Golden D. C., Ming D. W., Schwandt C. S., Morris R. V., Yang V., and Lofgren G. E. 2000. An experimental study on kinetically-driven precipitation of calcium-magnesium-iron carbonates from solution: Implications for low-temperature formation of carbonates in martian meteorite Allan Hills 84001. *Meteoritics & Planetary Science* 35:457–465.
- Golden D. C., Lauer H. V., Jr., Lofgren G. E., McKay G. A., Ming D. W., Morris R. V., Schwandt C. S., and Socki R. A. 2001. A simple inorganic process for formation of carbonates, magnetite, and sulfides in martian meteorite ALH 84001. *American Mineralogist* 86:370–375.
- Greenwood J. P. and McSween H. Y., Jr. 2001. Petrogenesis of Allan Hills 84001: Constraints from impact-melted feldspathic and silica glasses. *Meteoritics & Planetary Science* 36:43–61.
- Greenwood J. P. and McKeegan K. D. 2002. Oxygen isotope composition of silica in ALH 84001 (abstract). *Meteoritics & Planetary Science* 37:A58.
- Harvey R. P. and McSween H. Y., Jr. 1994. Ancestor's bones and palimpsests: Olivine in ALH 84001 and orthopyroxene in Chassigny (abstract). *Meteoritics* 29:472.
- Harvey R. P. and McSween H. Y., Jr. 1996. A possible high temperature origin for the carbonates in martian meteorite ALH 84001. *Nature* 382:49–51.
- Hutchins K. S. and Jakosky B. M. 1997. Carbonates in martian meteorites ALH 84001: A planetary perspective on the formation temperature. *Geophysical Research Letters* 24:819–822.
- Jull A. J. T., Eastoe C. J., Xue S., and Herzog G. F. 1995. Isotopic composition of carbonates in the SNC meteorites Allan Hills 84001 and Nakhla. *Meteoritics* 30:311–318.
- Jull A. J. T., Eastoe C. J., and Cloutd S. 1997. Isotopic composition of carbonates in the SNC meteorites, Allan Hills 84001 and Zagami. *Journal of Geophysical Research* 102:1663–1669.
- Kozioł A. M. and Brearley A. J. 2002. A non-biological origin for the nanophase magnetite grains in ALH 84001: Experimental results (abstract #1672). 33rd Lunar and Planetary Science Conference. CD-ROM.
- Langenhorst F. 2000. Mineral chemistry and structures in ALH 84001 (abstract #1866). 31st Lunar and Planetary Science Conference. CD-ROM.
- Leshin L. A., McKeegan K. D., Carpenter P. K., and Harvey R. P. 1998. Oxygen isotopic constraints on the genesis of carbonates from martian meteorite ALH 84001. *Geochimica et Cosmochimica Acta* 62:3–13.
- Mazurin O. V., Startsev Y. K., and Stoljar S. V. 1982. Temperature dependences of viscosity of glass-forming substances at constant fictive temperatures. *Journal of Non-Crystalline Solids* 52:105–114.
- McKay D. S., Gibson E. K., Jr., Thomas-Keprta K. L., Vali H., Romanek C. S., Clemett S. J., Chillier X. D. F., Maechling C. R., and Zare R. N. 1996. Search for past life on Mars: Possible relic biogenic activity in martian meteorite ALH 84001. *Science* 273:924–930.
- McKay G. A. and Lofgren G. E. 1997. Carbonates in ALH 84001: Evidence for kinetically controlled growth (abstract). 28th Lunar and Planetary Science Conference. pp. 921–922.
- McKay G. A., Mikouchi T., and Lofgren G. E. 1997. Carbonates and feldspathic glass in Allan Hills 84001: Additional complications (abstract). *Meteoritics & Planetary Science* 32:A87.
- McKay G. A., Schwandt C. S., and Mikouchi T. 1998a. Feldspathic glass and silica in Allan Hills 84001 (abstract). *Meteoritics & Planetary Science* 33:A102.
- McKay G., Mikouchi T., Schwandt C., and Lofgren G. 1998b. Fracture fillings in ALH 84001 feldspathic glass: Carbonate and silica (abstract #1944). 29th Lunar and Planetary Science Conference. CD-ROM.
- McSween H. Y., Jr. and Harvey R. P. 1998. An evaporation model for formation of carbonates in the ALH 84001 martian meteorite. *International Geology Review* 40:774–783.
- McSween H. Y., Jr. and Treiman A. H. 1998. Martian meteorites. In *Planetary materials*, edited by Papike J. J. Washington D.C.: Mineralogical Society of America.
- Mittlefehldt D. W. 1994. ALH 84001: A cumulate orthopyroxenite member of the martian meteorite clan. *Meteoritics* 29:214–221.
- Nyquist L., Bansal B. M., Wiesmann H., and Shih C. Y. 1995. Martians young and old: Zagami and ALH 84001 (abstract). 26th Lunar and Planetary Science Conference. pp. 1065–1066.
- Rekhson S. M., Heyes D. M., Montrose C. J., and Litovitz T. A. 1980. Comparison of viscoelastic behavior of glass with a Lennard-Jones model system. *Journal of Non-Crystalline Solids* 38-39:403–408.
- Romanek C. S., Grady M. M., Wright I. P., Mittlefehldt D. W., Socki R. A., Pillinger C. T., and Gibson E. K., Jr. 1994. Record of fluid-rock interactions on Mars from the meteorite ALH 84001. *Nature* 372:655–657.
- Romanek C. S., Gibson E. K., Jr., McKay D. S., Socki R. A., and Thomas K. L. 1995. Carbon- and sulfur-bearing minerals in the martian meteorite Allan Hills 84001 (abstract). *Meteoritics & Planetary Science* 30:567–568.
- Saxton J. M., Lyon I. C., and Turner G. 1998. Correlated chemical and isotopic zoning in carbonates in the martian meteorite ALH 84001. *Earth and Planetary Science Letters* 160:811–822.
- Schwandt C. S., McKay G. A., and Lofgren G. E. 1999. FESEM imaging reveals previously unseen detail and enhances interpretations of ALH 84001 carbonate petrogenesis (abstract #1346). 30th Lunar and Planetary Science Conference. CD-ROM.
- Scott E. R. D., Yamaguchi A., and Krot A. N. 1997. Petrological evidence for shock melting of carbonates in the martian meteorite ALH 84001. *Nature* 387:377–379.
- Scott E. R. D., Krot A. N., and Yamaguchi A. 1998. Carbonates in fractures of martian meteorite Allan Hills 84001: Petrologic evidence for impact origin. *Meteoritics & Planetary Science* 38:709–719.
- Scott E. R. D. and Barber D. J. 2002. Origin of magnetite in martian meteorite Allan Hills 84001 (abstract). *Meteoritics & Planetary Science* 37:A128.
- Segura T. L., Toon O. B., Colaprete A., and Zahnle K. 2002.

- Environmental effects of large impacts on Mars. *Science* 298: 1977–1980.
- Shearer C. S. and Adcock C. T. 1998. The relationship between the carbonate and shock-produced glass in ALH 84001 (abstract #1754). 29th Lunar and Planetary Science Conference. CD-ROM.
- Stöffler D. 2000. Maskelynite confirmed as diaplectic glass: Indication for peak shock pressures below 45 GPa in all martian meteorites (abstract #1170). 31st Lunar and Planetary Science Conference. CD-ROM.
- Thomas K. L., Gibson E. K., Keller L. P., McKay D. S., and Romanek C. 1996. Microanalysis of unique fine-grained minerals in the martian meteorite ALH 84001 (abstract). 27th Lunar and Planetary Science Conference. pp. 1327–1328.
- Treiman A. H. 1995. A petrographic history of martian meteorite ALH 84001: Two shocks and an ancient age. *Meteoritics* 30:294–302.
- Treiman A. H. 1998. The history of Allan Hills 84001 revised; Multiple shock events. *Meteoritics & Planetary Science* 33:753–764.
- Tromp R. M. and Hannon J. D. 2002. Thermodynamics of nucleation and growth. *Surface Reviews and Letters* 9:1565–1593.
- Turner G., Knott S. F., Ash R. D., and Gilmour J. D. 1997. Ar-Ar chronology of the martian meteorite ALH 84001: Evidence for the timing of the early bombardment of Mars. *Geochimica et Cosmochimica Acta* 61:3835–3850.
- Valley J. W., Eiler J. M., Graham C. M., Gibson E. K., Jr., Romanek C. S., and Stolper E. M. 1997. Low-temperature carbonate concretions in the martian meteorite ALH 84001: Evidence from the stable isotopes and mineralogy. *Science* 275:1633–1638.
- Warren P. H. 1998. Petrologic evidence for low-temperature, possible flood-evaporitic origin of carbonates in the Allan Hills 84001 meteorite (abstract). *Meteoritics & Planetary Science* 33:A162–A163.
- Woods T. L. and Garrels R. M. 1992. Calculated aqueous-solution-solid-solution relations in the low-temperature system CaO-MgO-FeO-CO₂-H₂O. *Geochimica et Cosmochimica Acta* 56: 3031–3043.
-